



Synchronous onset of the Messinian evaporite precipitation: First Mediterranean offshore evidence



Diana Ochoa^{a,*}, Francisco J. Sierro^a, Johanna Lofi^b, Agnès Maillard^c, Jose-Abel Flores^a, Mercedes Suárez^a

^a Geology Department, University of Salamanca, Plaza de la Merced s/n, E-37008 Salamanca, Spain

^b Géosciences Montpellier – UMR 5243, Université de Montpellier 2, Place E. Bataillo, 34095 Montpellier Cedex 05, France

^c Géosciences Environnement Toulouse (GET), Observatoire Midi Pyrénées, Université de Toulouse, CNRS, IRD, 14 avenue E. Belin, F-31400 Toulouse, France

ARTICLE INFO

Article history:

Received 18 February 2015

Received in revised form 9 June 2015

Accepted 29 June 2015

Available online 16 July 2015

Editor: D. Vance

Keywords:

Balearic Promontory

bedded unit

betic corridor

evaporites

Messinian Salinity Crisis

Primary Lower Gypsum

ABSTRACT

The Messinian Salinity Crisis (MSC) was a major ecological crisis affecting shallow and deep-water settings over the entire Mediterranean basin. However, the evolution of the MSC and its ecological impacts have mainly been explained on the basis of sediments from onshore outcrops. Lack of complete and physically connected records from onshore and offshore settings has inhibited comprehensive understanding of basin behaviour during the MSC. Herein we present a continuous record from an intermediate-depth basin on the Balearic Promontory that comprises late Tortonian–Messinian marls and evaporitic beds from the first MSC phase (i.e., Primary Lower Gypsum–PLG stage). Well-log and biostratigraphic data allow us establishing a large-scale calibration to the astronomical solutions, and to correlate pre-MSC sediments with classical rhythmic successions outcropping onshore. Thickness and characteristic sedimentary patterns observed in the offshore evaporitic records resemble those from marginal PLG sequences. Furthermore, seismic reflectors from a Bedded Unit (BU), which corresponds to an evaporitic interval according to well-to-seismic ties, are correlated with the onshore PLG sequences. This correlation constitutes the first attempt to link well-known marginal sequences with intermediate-depth offshore settings, which have previously only been studied through seismic imaging. Our time-calibration provides direct evidence supporting a synchronous onset of the PLG phase between onshore and offshore settings along the southwestern Balearic Promontory margin. Those BU reflectors, which were positively correlated to the PLG, were likely precipitated offshore the continental shelf at Messinian times. These results suggest that gypsum precipitation and/or preservation was not always limited to 200 m water-depths and could occur in non-silled basins. Finally, we only found a major erosion at the top of the PLG sequences, implying that the MSC drawdown occurred after the precipitation of the onshore lower evaporites. Studied sequences provide new insights into the PLG precipitation/preservation settings, as well as into the land-sea correlations of MSC units, and thus could potentially help refine current MSC models.

© 2015 Elsevier B.V. All rights reserved.

1. Introduction

During the latest Miocene, tectonic-driven processes triggered the closure of the Betic and Rifian gateways, which previously connected the Atlantic and the Mediterranean seas. Consequently, seawater exchange between these seas was reduced and Mediterranean waters became increasingly salty, leading to the precipitation of thick evaporite sequences (e.g. gypsum and halite) at different times and depocenters (see Roveri et al., 2014 and the references therein). A giant salt deposit, containing in volume

almost 5% of the salt of the world oceans (Ryan, 2008), was formed. This event, known as the Messinian Salinity Crisis–MSC, was rapid (5.97–5.33 Ma; Krijgsman et al., 1999; Manzi et al., 2013) and affected biological (e.g. Kouwenhoven et al., 1999; Sierro et al., 2003), chemical (De Lange and Krijgsman, 2010), and sedimentary processes in the Mediterranean Sea (CIESM, 2008; Roveri et al., 2014). At a global scale, the closure of these gateways would impacted the North Atlantic hydrography, by altering the exchange of water, heat, nutrients, and salt. Hence, it influenced the northern hemisphere's ocean circulation and climate (Rogerson et al., 2012).

Multiproxy studies have demonstrated that the crisis affected the complete Mediterranean basin. Nonetheless, the MSC evolu-

* Corresponding author.

E-mail address: diana.ochoa@usal.es (D. Ochoa).

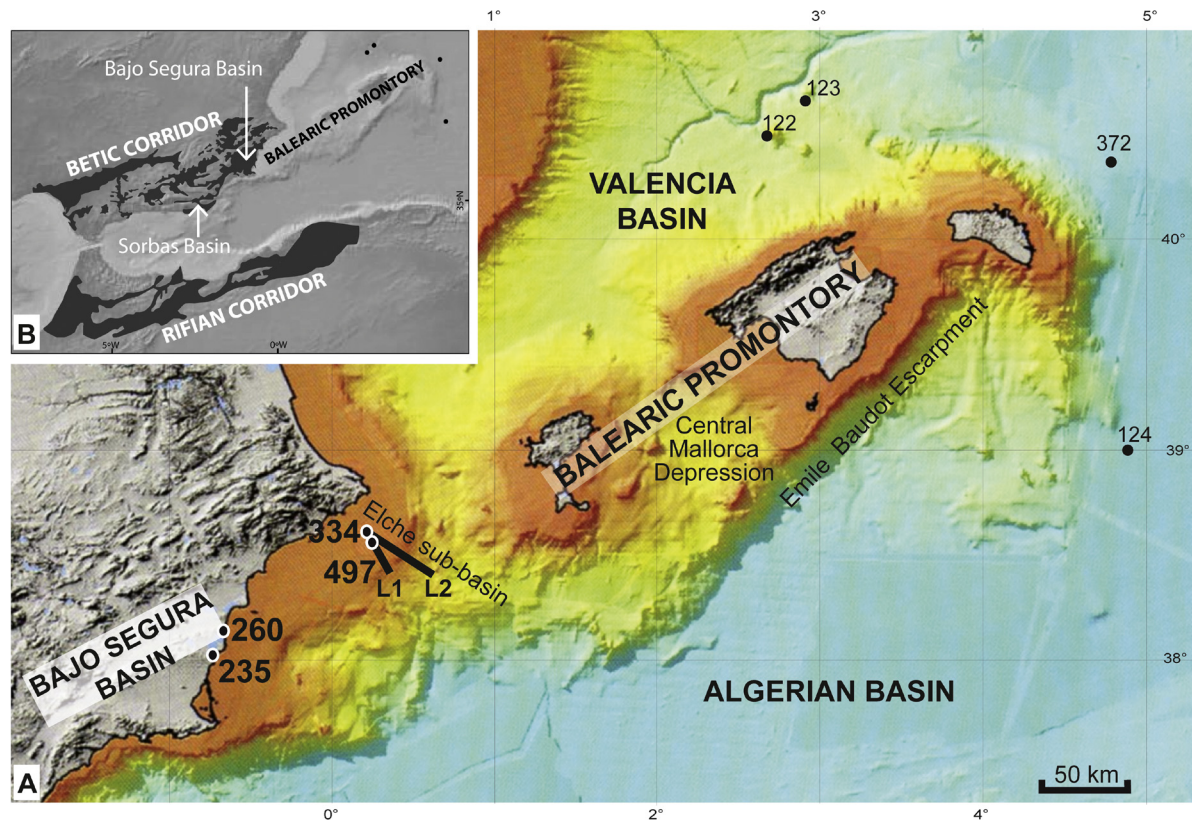


Fig. 1. A) Bathymetric map of the Balearic Promontory modified after Maillard and Mauffret (2013). Numbers indicate studied wells: 235-San Miguel-1, 260-La Mata, 334-Calpe, and 497-Muchamiel. SIMBAD seismic profiles (L1 and L2) shown in Fig. 8 are also located. B) Reconstructed Betic and Rifian gateways based on present-day location of onshore Late Miocene marine sediments. Location of Sorbas and Bajo Segura marginal basins is also shown.

tion has been traditionally explained by using observations and data from uplifted marginal areas. In onshore successions, three MSC-sedimentary units characterised by distinct evaporitic associations, are observed (see CIESM, 2008 and Roveri et al., 2014 and the references therein). These units can be roughly described as: primary lower gypsum (Lower Evaporites), followed by halite with clastic gypsum, ending in either brackish deposits (*Lago Mare*) or gypsum sequences (Upper Evaporites). By contrast, Messinian offshore stratigraphy mostly relies on seismic profiles. Three MSC-related seismic units have been identified in the deep Western Mediterranean basins (i.e., the Messinian trilogy of Montadert et al., 1970) based on their seismic facies and geometrical arrangements. This trilogy is formed by: the Lower Unit, the Mobile Unit consisting mainly of halite, and the Upper Unit that was partially drilled during some DSDP/ODP legs (Ryan et al., 1973; Montadert et al., 1970). However, the age and/or nature of these units endure unknown. Additionally, a fourth seismic unit, known as the Bedded Unit (BU), was also identified in some disconnected intermediate-depth basins (Driussi et al., in press; Lofi et al., 2011; Maillard et al., 2014). As a result of these different datasets, stratigraphic correlations between onland sequences and offshore intermediate-depth, and between intermediate and deep-basin seismic records are challenging. Establishment of land-sea correlations has been hampered by the lack of complete and geometrically connected stratigraphic records. Consequently, scenarios explaining the causes, progression and timing of the MSC remain controversial, as they are largely untested.

In this work, we focused on the first phase of the crisis, known as the Primary Lower Gypsum-PLG stage (5.971–5.61 Ma) (CIESM, 2008; Lugli et al., 2010; Manzi et al., 2013). This phase has been characterised by hypersaline conditions, causing the precipitation of gypsum at shallower settings (<200 m) and aplanktic dolomites

or black shales at deeper settings (<1000 m) (e.g. Dela Pierre et al., 2012; Hilgen and Krijgsman, 1999; Manzi et al., 2007; Lugli et al., 2010). Gypsum precipitation has been linked to precession-driven changes in climate (Krijgsman et al., 1999; Lugli et al., 2010; Manzi et al., 2013), and it is generally interpreted as only occurring at interconnected but silled subbasins with restricted water circulation (Lugli et al., 2010). High-resolution chronostratigraphic studies in pre-crisis sediments have indicated that the onset of this first stage was synchronous around the Mediterranean basin (Krijgsman et al., 1999).

Through the integration of biostratigraphic, logging and seismic data, here we investigated drilled-sediments from the Balearic Promontory that were recently associated with onshore PLG successions (Driussi et al., in press). We determined the timing of the PLG onset and established a reliable chronostratigraphic framework for offshore intermediate-depth settings (<1000 m) in the promontory, which allowed detailed correlations with Messinian onland shallow-water records (<200 m). Studied records have experienced relatively little syn- and post-MSC deformation and include a complete pre-MSC record directly connected to the Betic Corridor (Fig. 1). Thus, they were successfully time-calibrated, laterally connected with outcropping onshore sections, and their seismic expression was further extended basinwards. We demonstrated that PLG evaporites are present at current depths of up to 1000 mbsl along the promontory, and that they correspond to the seismic Bedded Unit reflectors from the southwestern promontory margin. Finally, by comparing our sequences with those from marginal onshore basins (Sorbas and Bajo Segura basins; Fig. 1A), we reconstructed the geological evolution of the southwestern Balearic Promontory margin before and during the PLG stage and discussed implications for the MSC. Comprehensive analyses on

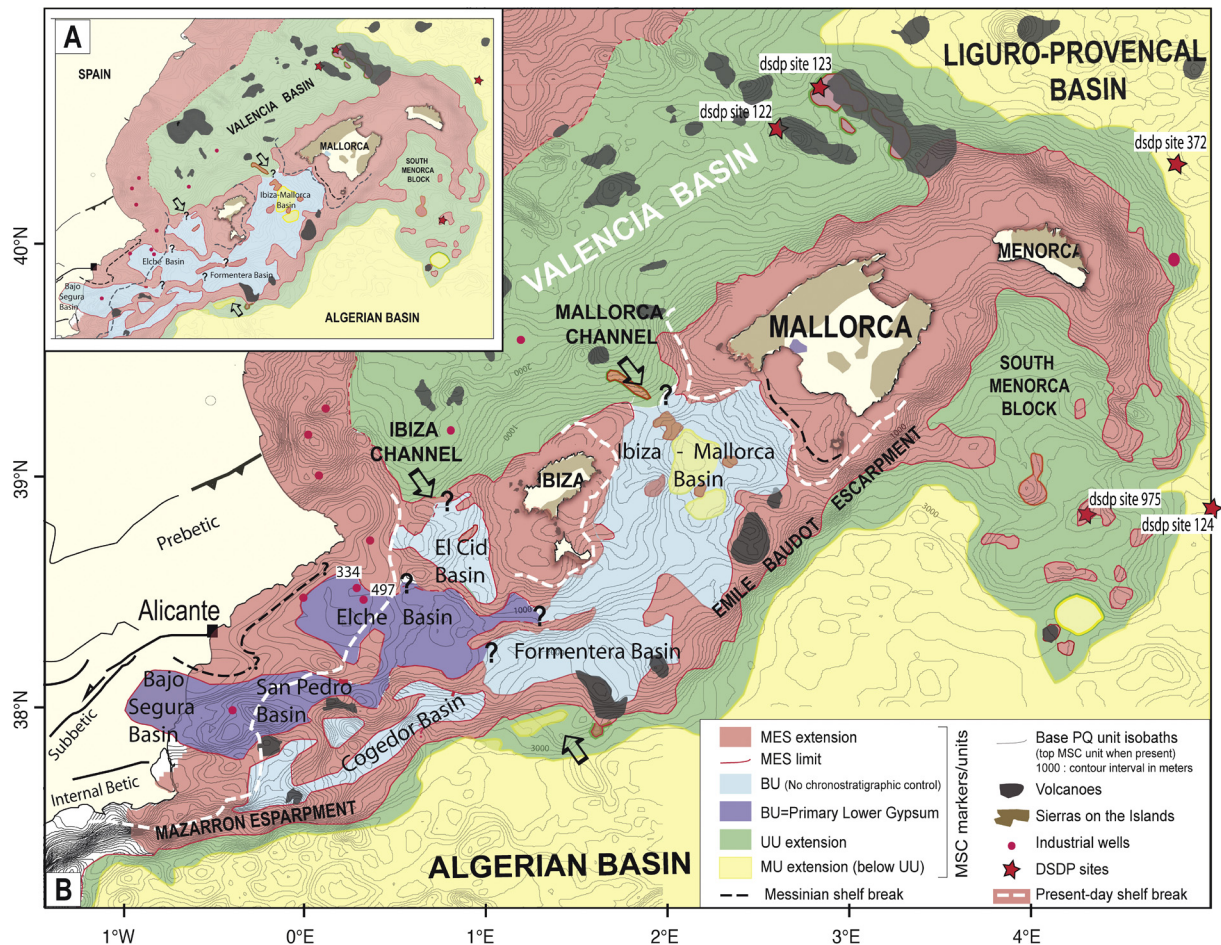


Fig. 2. A) Map showing present-day extent of the Bedded Units-BU (blue) over the Balearic Promontory. Seismic units from adjacent deeper basins correspond to the Upper Unit (green) and the Mobile Unit (yellow), both belonging to the deep basin Messinian trilogy. Extent of the Margin Erosional Surface-MES is shown in red. B) Map indicating confirmed presence of Primary Lower Gypsum-PLG (purple, after this study) and Bedded Units (in blue) over the Balearic Promontory. Note that modern-day Alicante continental shelf is significantly more prolonged than the reconstructed Messinian continental shelf (dashed grey line), and that confirmed PLG sequences extend further the Messinian shelf break along the Alicante area (Elche sub-basin). Studied wells (334-Calpe, and 497-Muchamiel) are indicated; note that during Messinian times both drills were located after the continental shelf. Base map has been modified from [Driussi et al. \(in press\)](#). (For interpretation of the references to colour in this figure legend, the reader is referred to the web version of this article.)

intermediate-depth offshore records are critical for expanding and testing current debates on possible MSC scenarios.

2. Messinian-related offshore records from the Balearic Promontory

The Balearic Promontory (BP) is bordered by the deeper Valencia and Liguro-Provençal basins to the north, and by the Algerian basin to the south (Fig. 1). It is the northeast offshore prolongation of the Betic Range, and connects with the onshore uplifted Betic Corridor through the Bajo Segura basin (Figs. 1, 2). As part of the Betic Range, the BP suffered extensional tectonism during the late Miocene, which promoted the opening of several intramontane basins (e.g., Sorbas and Bajo Segura basins) (Fig. 1A; [Acosta et al., 2004](#); [Maillard and Mauffret, 2013](#)). Onshore and offshore Mio-Quaternary rocks were accumulated under similar tectonic settings related to the transpressive Eastern Betic Shear Zone ([Alfaro et al., 2002](#)). Given that recent deformation only affects the area locally, sediments along the SW margin are relatively undeformed (Fig. 3).

Recently, a series of seismic units interpreted as MSC in age, were recognised along the BP. These units include the MSC-unit of [Driussi et al. \(in press\)](#) (Fig. 2A), and the BU and Slope units of [Maillard et al. \(2014\)](#). Following the nomenclature of [Lofi et al. \(2011\)](#), here they are grouped and will be referred to as the “*Bedded Units* (BU)”. The BU facies consist mainly of relatively continu-

ous sub-parallel reflections, which are geometrically disconnected from the MSC trilogy accumulated in the deep Western Mediterranean basins. Therefore their relative age cannot be established. Although BU facies resemble the ones of the Upper Unit (UU) from the Valencia basin ([Lofi et al., 2011](#); [Maillard et al., 2006](#)), their current isolation prevents reliable correlations with the UU ([Acosta et al., 2004](#); [Driussi et al., in press](#)).

Along the promontory, the BU deposits were accumulated in a series of sub-basins lying between 600–2000 m present-day water depths (Fig. 2; [Acosta et al., 2004](#); [Driussi et al., in press](#); [Maillard et al., 2014](#)). The paleo-connections among these sub-basins during the MSC remain uncertain ([Driussi et al., in press](#)). In general, basal BU reflections are conformably overlying pre-MSC sequences of variable thicknesses, while upper BU reflectors are locally bounded by an erosive surface, described as the Top BU Erosional Surface. The BU sequence is overlaid by a thick Plio-Quaternary sedimentary cover, which often displays transparent seismic facies (Fig. 3). According to well-to-seismic ties, the BU present in the southwestern BP margin is thought to correspond with the onshore PLG deposits ([Driussi et al., in press](#)), but their age has not been confirmed yet. Moreover, the spatial variability of the BU at the scale of the promontory, in terms of lithology and age, also still needs to be addressed. For instance, in the central Balearic depression, at least two generations of BU (one including a thin halite layer) have been evidenced ([Maillard et al., 2014](#)). Furthermore,

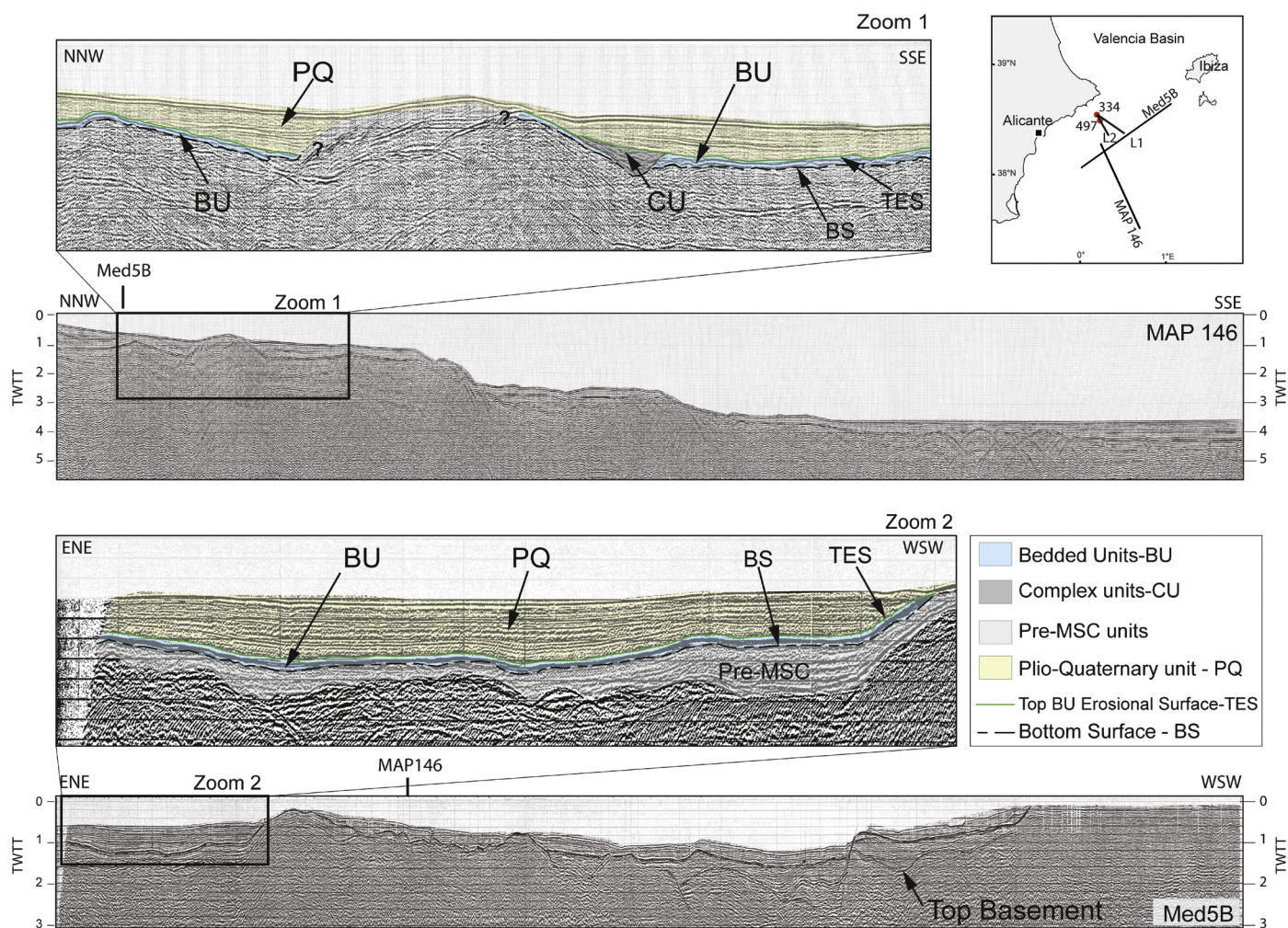


Fig. 3. Industrial seismic lines along the southwestern margin of the Balearic Promontory. Lines show poorly deformed Neogene deposits. Expression and lateral extension of the Beeded Unit are highlighted. Note that seismic profiles cross each other. SIMBAD seismic profiles (L1 and L2) shown in Fig. 7 are also located. (For interpretation of the references to colour in this figure legend, the reader is referred to the web version of this article.)

Maillard et al. (2014) proposed that most of the BU reflectors from the BP are pre-UU, and only the upper most reflectors find at some topographic lows could be equivalent to the UU.

3. Well data and methodology

3.1. Well-log data and seismic ties

For this study, we used lithological reports, logging data and cutting samples from two oil-industry wells drilled on the southwestern BP margin (497-Muchamiel and 334-Calpe; Fig. 1, Appendix A). These drills are currently located within the continental platform; but were offshore the shelf break during Messinian times (Fig. 2A). Complementary data from the Bajo Segura Basin (BSB) were obtained from two onshore wells (260-La Mata and 235-San Miguel-1; Fig. 1, Appendix A).

Available downhole logs include gamma-ray (GR), sonic (slowness) and resistivity. GR data provide a measure of the total gamma-ray emissions of the formation, allowing identification of main sedimentary units. The GR signal generally increases in magnitude with shale content. Carbonate, non-radioactive sands, and clean gypsum/halite deposits typically have low GR values. Resistivity logs provide information on the electrical resistivity of formations at different penetration depths. Electrical resistivity is driven by porosity, permeability, saturation and interstitial fluid salinity. High resistivities are typically encountered in gypsum,

whereas low ones characterise clays. The sonic log measures the travel time of sound through the rock. Evaporites usually have much shorter transit times (low slowness) than moderately consolidated sediments (Ellis and Singer, 2007).

Mineral phases from the Muchamiel borehole were also determined by X ray diffraction-XRD (Appendix B). Additionally, two high-resolution seismic reflection profiles acquired during the SIMBAD/2013 cruise (Appendix A) were tied to offshore wells (Fig. 1B). Time-depth conversions were calculated using average velocities derived from sonic logs and cross-validated with borehole data (Appendix C).

3.2. Micropaleontological analyses

We performed quantitative and qualitative foraminiferal analyses in 86 samples. At least 200 specimens from the > 150 μm fraction were counted per split sample (Appendix D). Taxonomic identification and chronological age models followed previous frameworks proposed for the Mediterranean Sea (e.g. Hilgen et al., 1995; Hüsing et al., 2009; Krijgsman et al., 1999; Sierro et al., 2001).

3.3. Time series analyses

We performed Continuous Wavelet and REDFIT analyses on borehole data for detecting significant periodicities and their time/depth dependence and significance (see Appendix E). Cross-

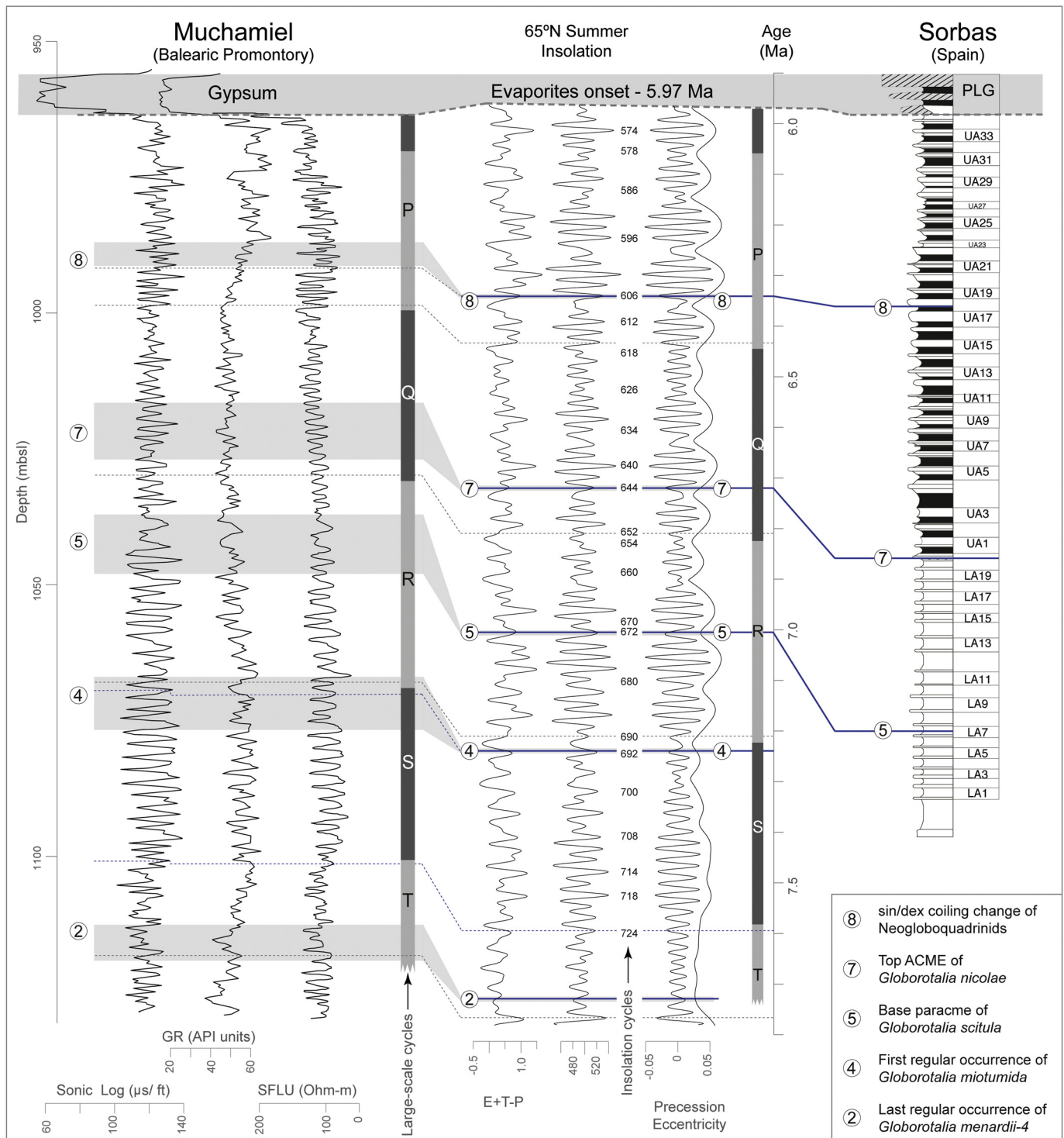


Fig. 5. Astronomical tuning of pre-evaporite sonic (slowness), gamma-ray and resistivity logs of the 497-Muchamiel well with the combined ETP (eccentricity, negative precession) and 65°N summer insolation curve of La2004_(1,1) (Laskar et al., 2004). Biostratigraphic events used as reference levels are: (2) Last Regular Occurrence of *Globorotalia menardii-4* (sinistral); (4) First Regular Occurrence of *Globorotalia miotumida*; (5) Base paracme of the *Globorotalia scitula*; (7) Top ACME of *Globorotalia nicolae*; (8) sinistral/dextral coiling change of *Neogloboquadrinids*. Thick dashed lines show correlation to key beds from the Sorbas section (Manzi et al., 2013; Sierro et al., 2001). Precessional cycle numbers after Lourens et al. (1996).

sum/marl intercalations produce fluctuating, high amplitude log records allowing recognition of 8 to 12 individual evaporite layers. Similar resistivity readings (characteristic shapes) are recorded in the Betics (Soria et al., 2008) and the Adriatic regions (Chielmi et al., 2013; Roveri et al., 2005). In the Muchamiel well, the uppermost part of this facies shows a singular pattern (~878–921 mbsl; Fig. 4). Here the logs display lower amplitude and frequency variability, with GR, sonic and resistivity generally peaking at lower

values compared to the evaporitic interval below. The evaporitic nature of this interval is confirmed by drilling reports, cuttings lithology and XRD analyses (Appendix B). There is no evidence of *in-situ* foraminifera within this facies.

4.1.3. Post-evaporitic facies

At the base, the post-evaporitic succession consists of ~35 m of well-cemented calcareous clayey limestones, without presence

of evaporite mineral phases (Appendix B). The GR and sonic logs show an increasing-upwards trend towards positive values, with attenuated amplitude (Fig. 4). Light-grey soft clays with pyrite and abundant foraminifera overlie these limestones. Upper clays are typical open-marine deposits.

4.2. Biostratigraphy and biochronology

Foraminifer preservation and abundance are overall good to moderate in the pre-evaporitic sediments, decreasing only towards the evaporite contact. We identified 8 planktic foraminifer bioevents spanning from the Tortonian to the Messinian (Fig. 4). The uncertainty on the depth location of bioevents can be as high as 6 m, depending on the nature and resolution of the samples (grey intervals; Figs. 4, 5). Because downhole contamination could displace *First Occurrence* (FO) events, biostratigraphic dating was only based on *Last Occurrence* (LO) bioevents. Nonetheless, some relevant FO events are indicated for reference (Fig. 4; Appendix D).

Identified bioevents and their stratigraphic positions fit well with previous high-resolution Mediterranean chronostratigraphic models (e.g. Hilgen and Krijgsman, 1999; Husing et al., 2009; Krijgsman et al., 1999; Sierro et al., 2001). In the lower part, *Globorotalia menardii-4* is continuously present and abundant, but its abundance decreases upwards until disappearance. This abundance pattern permits correlation with the Italian Corvi section, where decrease and disappearance of *G.menardii-4* have been dated at 7.72 Ma and 7.51 Ma, respectively (Husing et al., 2009). Higher in the succession, *Globorotalia miotumida* is commonly found along with *Globorotalia scitula* (sinistral and dextral forms). The base of the paracme of *G.scitula* occurs at ~1030 mbsl in Muchamiel. This paracme has been calibrated at 6.98 Ma (Husing et al., 2009; Sierro et al., 2001). *G.nicolae* is found in a short interval, its LO was identified around ~1020 mbsl in Muchamiel. The LO of *G.nicolae* has been dated at 6.8 Ma, marking the Lower/Upper Abad boundary in the Sorbas basin (Sierro et al., 2001). In the same interval we found the FO of *Rectouvigerina cylindrica*, a benthic taxon that also appears around 6.8 Ma (Krijgsman et al., 2006; Sierro et al., 2001). Above the FO of *R.cylindrica*, we identified a change in the benthic foraminiferal assemblage. Genera such as *Uvigerina*, *Bolivina* and *Brizalina* gradually become more abundant upwards, until they dominate the assemblage below the evaporite beds. The last bioevents recorded are the sinistral to dextral coiling change of Neogloboquadrinids (6.35 Ma) and an influx of *Turborotalita multiloba* (Fig. 4; Appendix D). An increase on abundance of *Orbulina universa* also occurs towards the top of the pre-evaporitic facies. A comparable increase was observed in the Sorbas basin (UA14 onwards) (Sierro et al., 2003).

A first approximation to the minimum time span in the pre-evaporite record was estimated using the age-depth location of the LRO of *Globorotalia menardii-4* and LO of *Globorotalia nicolae* (bioevents 2 and 7; Figs. 4, 5). These events are reliable and have been dated in other Mediterranean basins at 7.72 and 6.72 Ma, respectively (Hilgen et al., 1995; Husing et al., 2009; Krijgsman et al., 1999; Sierro et al., 2001). We therefore calculated an average sedimentation rate of 8.84 cm/kyr and average cycle duration of 18.1–23.3 kyr for cycles of 2.1–1.6 m. The established biostratigraphic control, the regularity and pattern of log alternations, plus the estimation of time per cycle suggests that observed log oscillations correspond to astronomically-forced cycles.

No biostratigraphic framework was established for the evaporite sequence since there are no *in situ* foraminifera. By contrast, post-evaporitic sediments contain typical Pliocene marker taxa such as *Sphaerodinellopsis* spp., *Globorotalia margaritae*, and *Globorotalia punctulata*, as well as abundant and diverse open-marine benthic forms. However, a late Messinian age for the lowermost post-evaporitic sediments cannot be completely excluded.

5. Age control of pre-evaporite sediments

In order to tune a stratigraphic sequence to the astronomical target curve (Laskar et al., 2004) it is necessary to establish a phase relationship between the sedimentary processes and the orbital cycles. Hypotheses linking the sedimentary response to orbital forcing are well established for Neogene successions in the Mediterranean Sea and eastern Atlantic Ocean (e.g. Lourens et al., 1996; Sierro et al., 2000), where sapropels or equivalent CaCO₃-depleted marls are interpreted as deposited during precession minima/summer insolation maxima, while homogeneous carbonate-rich marls correspond to precession maxima/summer insolation minima. As eccentricity modulates the precessional amplitude, at times of eccentricity maxima precessional cycles are more developed than those at eccentricity minima. Alternations of thin-thick layers correspond to additional precession/obliquity interference (Hilgen and Krijgsman, 1999; Sierro et al., 2000).

We interpreted the alternations in the gamma-ray, sonic, and resistivity logs of the pre-evaporitic successions as changes in the clay/silt and organic matter/carbonate content. Clay-rich sediments with higher organic content (high sonic and GR) may be equivalent to sapropelic layers, which formed at times of increased precipitation. Similar correlation between organic-rich layers and high GR has also been reported in sediments from the eastern Mediterranean (ODP-Site 967; Emeis et al., 1996). Silt/carbonate-rich sediments (low sonic and GR) are compatible with deposition under dry conditions, when runoff and terrigenous supply were reduced during precession maxima/summer insolation minima.

For calibration purposes, we used the 65°N summer insolation curve of La2004_(1,1) (Laskar et al., 2004), with present-day values for the dynamical ellipticity of the Earth and the tidal dissipation by the moon (Lourens et al., 1996). As a starting point, we used again the same bioevents: LRO of *G.menardii-4* and LO of *G.nicolae* (Fig. 5). When considering the age-depth of these bioevents as limits, we found roughly the same number of log oscillations (47) between bioevents as the ones seen in other astronomically tuned Mediterranean sections (46, cycles 724 to 644; Fig. 5). We then established a correlation between the 400-kyr eccentricity minima and the logs. Although their boundaries are not always distinct, patterns of large-scale (400-kyr) cycles can be distinguished due to the presence of weakly developed oscillations occurring during 400-kyr eccentricity minimum intervals (Fig. 5).

After the initial large-scale calibration, we attempted to correlate logs to the 100-kyr cyclicity. Individual identification of 100-kyr bundles is not particularly clear, especially in large-scale cycles P and S (Fig. 5). It is possible that the interference of obliquity and precession is obscuring the boundaries of 100-kyr cycles present in the interval S. Finally, we attempted to correlate general log patterns to the 65°N summer insolation curve (Fig. 5). Although, logs have almost the same number of alternations than the target curve, precessional- or obliquity-related patterns are not distinct. Consequently, we still are unable to provide a definite peak-to-peak correlation between the observed log patterns and the 65°N summer insolation curve.

To independently test our large-scale age model (i.e. a 400 kyr age model), we run a cross-spectral analysis of the 400-kyr tuned logs against the 65°N summer insolation curve of La2004_(1,1) (Laskar et al., 2004). Results show that all the logs exhibit significant variance in the precessional frequencies (Fig. 6). Logs and 65°N summer insolation signals are coherent (above 95% level) at the precession periods (19- and 23-kyr). Logs also show significant coherency at the obliquity 41-kyr and 54-kyr bands (Fig. 6). Coherence in the obliquity bands revealed in all three logs is particularly interesting because obliquity-driven cycles were not considered during the tuning as the sedimentary response to obliquity is not evident. Although, the correlation of precessional-scale cycles is

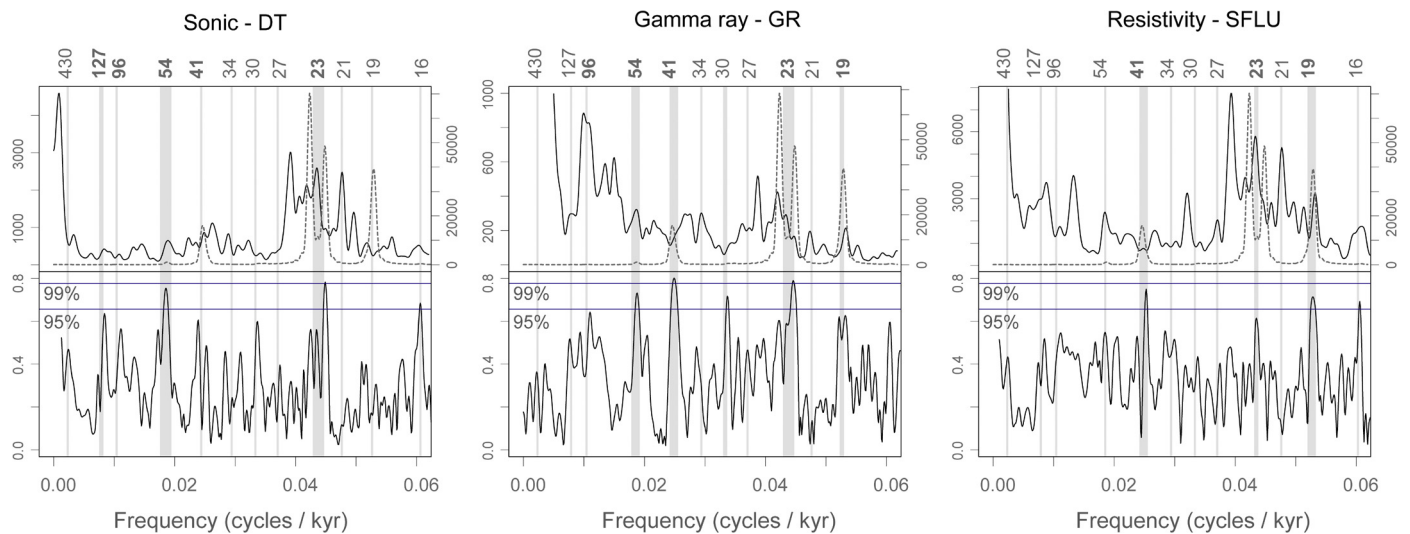


Fig. 6. Cross-spectral results for pre- evaporitic sediments from the 497-Muchamiel well. Analysis between sonic, gamma-ray and resistivity logs in time domain (tuned at 400-kyr scale) against the 65°N summer insolation curve of La2004_(1,1) (Laskar et al., 2004). Top panel shows normalised density spectra of log data (solid line) and summer insolation (dashed line). Spectral densities are plotted on log scales, left axis for well-log data and right axis for summer insolation. Bandwidth is 0.00149. Bottom panel shows coherency plot, horizontal lines indicate 99% and 95% confidence levels of non-zero coherency (0.78 and 0.66, respectively). Frequencies at which peaks have more than 95% confidence are highlighted in each panel. Signals were linearly detrended and a Blackman–Tukey spectral method (with Bartlett window) was then performed.

prevented by the weak or even lack of expression of eccentricity patterns, periodicities revealed by the spectral analysis in the time domain (19, 23, 41, and 54-kyr) support an astronomical origin for the sedimentary cyclicity observed in the log records. In addition, established chronology is in good agreement with all the biostratigraphic events that were observed.

6. Pre- evaporitic evolution of the Balearic Promontory

Sedimentation along the southwestern margin of the Balearic Promontory (BP) during the late Tortonian occurred in open-marine conditions without evidence of restricted water circulation along the Messinian margin slopes, where both studied sites were located (Fig. 2; Driussi et al., in press). Calcareous clayey to silty prograding sequences infilled the deepest part of the promontory. Orbitally-driven climatic processes resulting in dry/wet alternations are reflected in the lithological patterns throughout the pre- evaporitic facies (Fig. 5). Observed cyclicity is continuous but bearing a heterogeneous expression. Oscillations decrease in amplitude and thickness upwards towards the onset of evaporite precipitation (Appendix E). This variation in sedimentary cyclicity indicates both a reduction in sedimentation rates and a change in total sediment supplied to the basin. For example, clay/organic content increases with time, as indicated by higher GR values (~50–60 API units) seen in the Muchamiel well from 1000 mbsl upwards (Fig. 5). The absence of coarse-grained detrital material indicates that the southwestern BP margin, although part of the Betic system, was not strongly affected by late Tortonian uplift (Krijgsman et al., 2006; Soria et al., 2001). Unlike the Eastern Betics, there is no biological or lithological evidence suggesting that the Tortonian Salinity Crisis (7.8–7.6 Ma; Krijgsman et al., 2000) influenced this area. There is also no indication of suboxic–anoxic conditions in the pre-MSC succession, as reported for Sicily, Spain, and Italy based on the presence of diatomaceous layers (e.g. Hilgen et al., 1995; Krijgsman et al., 2000). It is possible, however, that the nature and quality of available cutting sample material obscures evidence of short intervals of disrupted circulation.

A rapid and marked change in sediment supply and faunal assemblages occurred at 6.4 Ma (~995 and ~755 mbsl in Muchamiel and Calpe, respectively). At this time, benthic communities became rich in low-oxygen and stress-tolerant taxa (e.g. *Bolivina*,

and *Brizalina*), and planktic assemblages were almost dominated by *Orbulina universa* (Appendix D). Additionally, the combined increase in abundance of *Globigerinoides* spp and decrease of groups such as the Neogloboquadrinids also indicates oligotrophic conditions, mostly resulting from restricted water circulation. Similar responses in plankton communities have been reported for other shallow and deep Mediterranean basins (e.g., Kouwenhoven et al., 1999; Sierra et al., 2003). In the Sorbas basin, these responses are interpreted as climatic-driven alterations of the trophic structure and water column mixing, which were amplified with increasing restriction of the basin (Sierra et al., 2003). Our data show that similar progressive deterioration of pelagic ecosystems is also reflected at intermediate-depth settings. Finally, evaporite precipitation started after these changes in water chemistry and circulation.

7. The bedded unit: offshore expression of the primary lower Gypsum in the southwestern BP margin

Tuning of precessional-driven pre- evaporitic marls revealed that open-marine sedimentation ceased circa 5.97 Ma (Fig. 5), which coincides with the evaporite onset proposed for marginal Mediterranean basins (e.g. Hilgen and Krijgsman, 1999; Krijgsman et al., 1999, 2001; Manzi et al., 2013; Sierra et al., 2001). The marl/evaporite transition appears as a continuous sedimentary contact along the southwestern BP margin. Consequently, the onset of known onshore Primary Lower Gypsum-PLG and studied offshore evaporites successions appears to be coeval. Established chronostratigraphic framework allows a direct correlation between onshore PLG sequences and offshore evaporites, which can be seismically followed basinwards (see Fig. 2B). Calibration and dating of these logs represent the first direct evidence from an offshore intermediate-depth basin, which supports a synchronous gypsum precipitation along the southwestern BP margin and onshore Bajo Segura basin (BSB).

We reviewed the evaporite stratigraphic record at the BP and contiguous BSB by taking advantage of evaporite physical properties. As evaporites are non-porous and electrically non-conductive materials, they are characterised by high resistivity values (>1000 Ωm), high velocities (~52 μs/ft), and generally low GR values (0 API units). In comparison, shales record low resistivity (5–30 Ωm) and high GR readings (~80–300 API units) (Ellis and Singer, 2007). In this work, individual evaporite beds

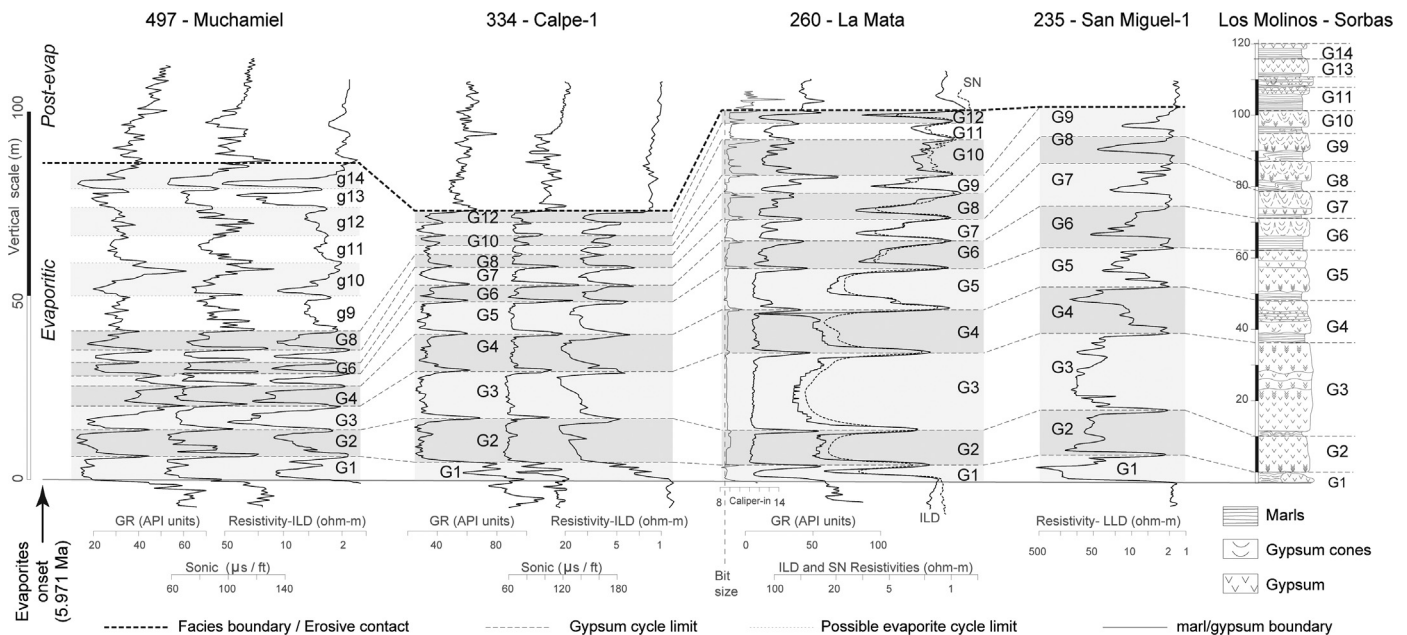


Fig. 7. Evaporite bed identification and correlation of log sequences between offshore wells from the Balearic Promontory and the Bajo Segura basin. Bed-to-bed correlation with the Yeseres member from the Sorbas basin is also shown. Sorbas stratigraphy after [Dronkert \(1976\)](#), [Krijgsman et al. \(2001\)](#), and [Manzi et al. \(2013\)](#). Individual evaporite beds are primarily identified based on resistivity logs. Note similarities on cycle relative thicknesses and stacking patterns between wells. Cycles noted as “G” are more evident, than those identified as “g”. All sequences are plotted using the same vertical scale. Post-evap: Post-evaporitic facies.

were primarily identified based on their resistivity characteristics ([Fig. 7](#)).

The PLG sequences both offshore and onshore show clear cyclic patterns with 8 to 14 gypsum/marl alternations ([Fig. 7](#)) and an increasing thickness towards the more proximal settings. In Muchamiel, evaporite/marl cyclicity can be unambiguously defined from the base up to cycle G8. From this point upwards, bed characterisation, thus cycle counting, is challenging because log spikes are less sharp. In [Fig. 7](#), well-defined beds are marked as “G”, while more uncertain beds are indicated with “g”. As XRD analyses and drilling report confirm the presence of gypsum phases above cycle G8 ([Fig. 7](#); [Appendix B](#)), it was possible to recognise 14 evaporite/marl cycles in Muchamiel. The last two cycles (g13 and g14; [Fig. 7](#)) are distinct and they point to the presence of two evaporite layers that are slightly more developed than the previous ones. These last developed gypsum beds may correlate with the two uppermost beds from the Sorbas basin, which locally appear thicker and more continuous than underlying gypsum beds ([Dronkert, 1976](#); [Krijgsman et al., 2001](#)).

In San Miguel-1 well, we identified 9 beds, in agreement with previous works ([Lugli et al., 2010](#); [Soria et al., 2008](#)). PLG successions from Calpe and La Mata wells are remarkably similar and 12 couplets are recognised. However, some authors suggest the presence of 15 gypsum beds in La Mata based on lithology and neutron log records ([Lugli et al., 2010](#)). Discrepancy between cycle numbering occurs at cycle G10 ([Fig. 7](#)). This level is characterised by up to four small-scale peaks in the GR and neutron logs, with deep- and shallow-resistivity readings that smoothly replicate these peaks. Caliper data show local borehole enlargement at same levels ([Fig. 7](#)). We interpreted it as only one evaporitic level, which contains fine-grained carbonate interbedded layers. This lithology would be prone to widening of the borehole by differential solubility, thus producing high GR, sonic and neutron values while maintaining relatively high resistivity readings. The same type of lithology has been recognised as occurring after cycle six in PLG sections from Italy, Sicily and Spain ([Krijgsman et al., 2001](#); [Lugli et al., 2010](#)) and, it is therefore plausible that it should also occur on the promontory.

Comparison of these sequences with other Mediterranean PLG successions revealed remarkable similarities in vertical stacking patterns and bed thickness ([Lugli et al., 2010](#)). PLG sequences display a first thin cycle, cycles 2 to 4 are thick, pure and well-expressed, and from the sixth cycle onwards gypsum beds are less pure and contain more clay/carbonate ([Fig. 7](#)). In particular, resistivity logs from La Mata and San Miguel-1 wells show a decreasing-upwards trend, suggesting a transition from homogeneous and well-developed evaporite beds (cycles G2–G5) to more heterogeneous, less pure gypsum layers with massive gypsum at the base that become more marly towards the top (cycles G6–G9). Since the same stratigraphic pattern has been documented across the Mediterranean basin, it reflects regional hydrological dynamics rather than local changes in accommodation space/evaporite loading. Some differences between the onshore and offshore PLG successions are also observed. Firstly, cycles from proximal sites (Sorbas and Bajo Segura basins) are considerably thicker than their correlative equivalents in the Calpe and Muchamiel wells ([Fig. 7](#)). A similar basinwards thinning of the PLG sequences was reported for the Tertiary Piedmont basin in Italy ([Dela Pierre et al., 2012](#)). Additionally, assuming that gypsum cycles are strictly precessionally controlled, we observed a basinward-decrease in cycle thickness of the interbedded marls from cycle G6 onwards. Gypsum beds in onshore sequences contain relatively more marls within each evaporite cycle than their equivalent offshore cycles, as evidenced by the higher GR logs. Note that we refer to the marl/carbonates simultaneously accumulated with gypsum, not to the interbedded marls. This reduction in marl content of the gypsum beds could be the result of reduced detrital input in more distal settings during first MSC-stage. Although this feature is seen in the offshore wells, it is not yet clear whether it is a local or basin-wide phenomenon.

To date, the most complete PLG sequence has been described for the northern Apennines (Vena del Gesso); where 16 cycles are recognised (e.g., [Lugli et al., 2010](#)). According to this, none of the evaporite successions studied on the BP is complete. Assuming accurate counting, at least 2–4 cycles are missing in the offshore wells, while 4–7 in the onshore sites. This suggests that a

post-evaporitic erosive event capped the topmost part of the PLG sequence along the BSB and the BP. Onshore works in the BSB have documented this erosive surface as the end-Messinian unconformity (e.g., Corbi et al., 2010; Soria et al., 2005, 2008). Similarly, seismic profiles reveal a post-evaporitic erosion surface, regarded as the Top BU Erosive Surface (e.g. Acosta et al., 2004; Driussi et al., *in press*; Maillard et al., 2006). Onshore and offshore paleontological data corroborate the erosion by indicating that the overlying marls were deposited during the early Pliocene (Corbi et al., 2010).

High-resolution seismic profiles have revealed the presence of the Bedded Unit-BU along the BP (Driussi et al., *in press*). Here, BU reflectors are distributed in sub-basins disconnected today by topographic highs (Fig. 2A). At the Muchamiel and Calpe drilling sites (Elche sub-basin), the BU is also observed on the tied-seismic profiles. The BU is found between ~0.6–1.5 stwtt, and is characterised by internal bedded reflectors (Driussi et al., *in press*). Depth-to-time conversions of borehole data show that the PLG unit fits in depth with the BU seismic unit (Fig. 8; Appendix C). The basal contact of the BU is well-expressed and without evidence of erosion (Driussi et al., *in press*), supporting our interpretation of a non-erosive sedimentary contact between pre-MSC marls and evaporites (Fig. 8). High-resolution profiles often show that the three lowermost reflectors of the BU are of higher amplitude. These are likely to correspond to the lower well-developed gypsum cycles (G2 to G4) of the PLG. Profiles also show an erosive contact between the BU and the overlying Plio-Quaternary sediments. Erosion is recognisable mainly by truncation of the underlying reflectors forming the BU (Fig. 7). Since (i) we do not recognise any offshore erosive transition between the pre-evaporitic marls and the PLG, and (ii) we can correlate the erosional unconformity at the top of the gypsum with the onshore end-Messinian unconformity. We thus consider that the Marginal Erosion Surface (MES) and the Top BU erosive surface (and by extension the end-Messinian onland unconformity) correspond to the same chronostratigraphic surface in the Elche sub-basin of the BP. However this may not be the case for stepped sub-basins or in deeper settings on the promontory.

Dating of the studied offshore evaporite sequences and well-to-seismic ties allow establishing a reliable correlation between the PLG and the Bedded Unit along the southwestern BP margin. Since the BU crossed in the studied boreholes can be traced offshore throughout the southwestern margin of the promontory (Fig. 2B), we can demonstrate that the PLG is present today from onshore to present water depths of near 1000 mbsl. In those connected areas a synchronous precipitation can be acknowledged, and thus the presence of the first gypsum (or strong BU reflector) can be used as a reliable chronological marker indicating the PLG evaporation onset. By contrast, the presence of PLG in the eastern and deeper parts of the BP (e.g., the Central Mallorca Depression-CMD) cannot be confirmed because of the lack of continuity between the Bedded Units reflectors (Fig. 2B), although similar seismic facies are observed throughout the promontory (Fig. 2A), and in the Upper Unit from the deeper Valencia Basin (Fig. 2B). At the CMD, the Bedded Units appear interbedded with salt-like reflectors (Maillard et al., 2014), resembling very much the deep-basin trilogy (Montadert et al., 1970) or even the onshore records from Sicily (Roveri et al., 2008). Consequently, further review of the age and lithological character of the Bedded Unit at the CMD remains critical to understanding the timing and evolution of the MSC in Western Mediterranean deep basins.

Mapping of the MSC-related sediments along the promontory (i.e., the confirmed PLG sequences and Bedded Units; Fig. 2B) indicates that either gypsum was only precipitated in certain basins or it was completely removed during the sea-level fall causing the MES (i.e., Top-BU erosional surface). Finally, the present-day extension of the confirmed PLG also shows that gypsum beds precipi-

tated offshore the Messinian continental shelf reaching the margin slope (Fig. 2B). Therefore it indicates that PLG precipitation was not restricted to the continental shelf. This evidence questions current models, in which gypsum precipitation and/or preservation would be restricted to either silled or shallow basins (<200 m).

8. Timing of the major Mediterranean base-level drawdown

One of the main controversies regarding the MSC is related to the occurrence, timing and amplitude of a major sea-level change during the crisis. Though the presence of a widespread Marginal Erosional Surface (MES) has been used as evidence supporting a high-amplitude drawdown, its chronostratigraphic position is largely debated across marginal basins (CIESM, 2008; Lofi et al., 2011; Ryan and Cita, 1978). In the western Mediterranean, debate results from the lack of clear stratigraphic and geometric relationships between pre- and post-evaporitic deposits, PLG sequences, and carbonate platforms (Terminal Carbonate Complex). Consequently, in the last decades at least three different MSC scenarios have been debated according to the MES position. The first model proposes that the MES occurs between the Tortonian–Messinian marls and the PLG with a discontinuity of at least 300 kyr (Braga et al., 2006; Martin and Braga 1994; Riding et al., 1998). In this context, the PLG would postdate the main Mediterranean desiccation event and the deep basin halite. In contrast, a second hypothesis places the MES on top of the PLG, predating the main sea-level fall and the deep basin evaporites, but partly coeval with the marginal carbonate platforms (CIESM, 2008; Roveri et al., 2009). A third scenario suggests a continuous sedimentation in some marginal basins during Tortonian–early Messinian times (e.g. Sorbas; Fortuin et al., 2000; Krijgsman et al., 2001), with an erosion phase occurring either at ~5.5 Ma or after the uppermost Messinian continental deposits (Clauzon et al., 1996; Cornée et al., 2004). In both cases, PLG precipitation predates the Mediterranean drawdown.

According to our chronostratigraphic framework for the southwestern BP margin, the offshore transition between the Tortonian–Messinian marls and the PLG sequences corresponds to an abrupt, but non-erosive contact (Figs. 5, 8), whereas the PLG/Pliocene marl transition is erosional (Figs. 7, 8). Differences in the total number of gypsum cycles, the erosive nature of the top-most BU reflectors shown by seismic profiles, and the presence of overlying Pliocene marls confirm the existence and stratigraphic placement of this erosion event, which occurred after the PLG (at least after cycle 12) and before 5.3 Ma. Consequently our data support the presence of only one large unconformity, located at the top of the PLG and thus post-dating the first MSC-stage. Basin-wide correlation of this erosion surface indicates that the onshore end-Messinian unconformity (in the BSB; Soria et al., 2005, 2008) and the offshore top BU erosive surface correspond to the same chronostratigraphic surface. The offshore extension of this unconformity corresponds with the MES, which is related with a major sea-level fall affecting the entire Mediterranean during the second-MSC stage (CIESM, 2008; Roveri et al., 2014). Consequently, we rule out the hypothesis of a major sea-level fall occurring before or at the onset of PLG precipitation. Nonetheless, we have not enough evidence to either support or exclude other proposed models.

This interpretation of a continuous transition at the PLG onset is in agreement with previous field observations and chronostratigraphic control from several Mediterranean basins, including the Sorbas basin (e.g., CIESM, 2008; Manzi et al., 2013; Roveri et al., 2014). However, it contrasts with data from the contiguous BSB where two erosive levels bounding the gypsum beds (or coeval proximal sediments) have been defined (Corbi et al., 2010; Soria et al., 2005; Soria et al., 2008). The basal erosion located below the PLG, referred as the intra-Messinian erosive surface, is consid-

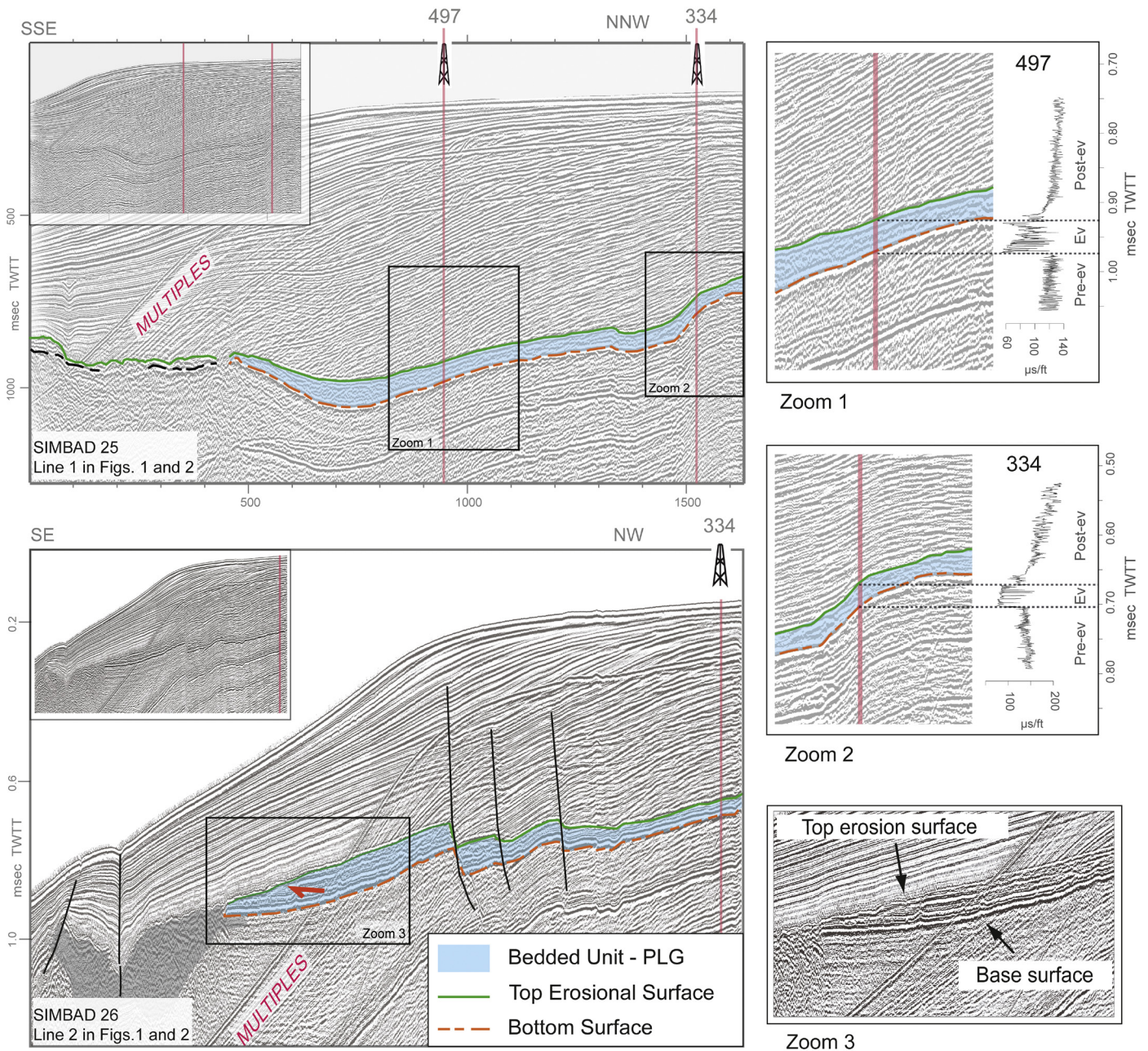


Fig. 8. Seismic profiles (SIMBAD lines 25 and 26, Tethys-II) across the southwestern margin of the Balearic Promontory (Elche sub-basin). Bedded Unit reflectors (BU) are highlighted in blue. Dashed and continuous lines at base and top correspond to the Bottom Surface and Top BU Erosional Surface, respectively. Vertical red lines indicate location of 497-Muchamiel and 334-Calpe wells. Zooms 1 and 2 show seismic facies and corresponding well-log facies in each drill-site. Note that BU reflectors correlate well with the drilled evaporite sequences. Zoom 3 shows non-erosive basal contact and a clear erosive contact at the top of the BU unit (i.e. PLG sequence). Bottom Surface corresponds to pre-MSC/evaporite transition while Top BU Erosional Surface marks the evaporite/post-evaporitic marls boundary. Post-ev = Post-evaporitic, Ev = Evaporitic, and Pre-ev = Pre-evaporitic sequences. Vertical scale is given in ms TWTT. Details of the seismic system configuration are found in Appendix A and [Driussi et al. \(in press\)](#). (For interpretation of the references to colour in this figure legend, the reader is referred to the web version of this article.)

ered to be a low-stand erosion surface, resulting from a large-scale sea level fall ([Soria et al., 2008](#)). However, south of the BSB, in less proximal settings, continuous marine sedimentation prevails at least to the base of the Gilbert Chron (6.03 Ma) according to magnetostratigraphic data ([Soria et al., 2008](#); [Corbi et al., 2010](#)). As a consequence, the intra-Messinian erosion would represent a hiatus of maximum 65 kyr, while basinward there is no seismic evidence of a pre-evaporitic unconformity ([Fig. 8](#); [Driussi et al., in press](#); [Martínez del Olmo, 2011](#)). Consequently this erosive phase preceded the evaporite onset and may have been the result of a relatively limited sea-level fall affecting only local marginal areas. [Cornée et al. \(2004\)](#) identified analogous erosive surfaces in car-

bonate platforms from marginal basins in Morocco, Algeria and Spain. They are coeval and have also been interpreted as marine planation surfaces resulting from low-amplitude sea level lowering.

9. Conclusions

We study the biostratigraphic record of two sedimentary successions from the southwestern BP margin (Elche sub-basin), which include a thick marly unit overlain by several evaporitic beds. Well-log alternating patterns, reflecting changes in clay/silt supply, were found to be mainly precessional-controlled sedimen-

tary cycles. Log patterns were therefore used to tune the succession to the astronomical curve. Despite some misfits at the precessional scale, the general pattern matches the astronomical target curve and the sedimentary expression from coeval reference sections on land. Time-calibration indicates that pre-evaporitic marls were continuously deposited during Tortonian–Messinian times, and transition to evaporitic beds occurred at 5.97 Ma. Additionally, vertical stacking patterns and internal features of individual gypsum beds allow us to correlate them with onshore well-log records and outcropping successions. Established tuning and correlations provide direct evidence supporting a synchronous evaporitic onset in an intermediate-depth setting, and confirm that no significant sea-level drawdown occurred before or during the PLG stage. Well-to-seismic ties reveal that offshore evaporitic beds correspond with the Bedded Unit along the southwestern BP margin (Fig. 2B). Nonetheless, this chronostratigraphic framework still needs to be demonstrated in other stepped sub-basins and/or deeper settings. Seismic and biostratigraphic data indicate that the limit between the PLG and overlying Pliocene marine marls is erosional. This erosive surface is interpreted as a drawdown phase during the second MSC-stage. From a chronostratigraphic point of view, it corresponds to the widespread margin erosional unconformity (MES) that can be traced from continental records down to the pinch out of the evaporite trilogy in the deep basin. This erosive phase could have removed the MSC-related sediments accumulated along the Messinian platforms and topographic highs. Finally, basinward extension of the confirmed PLG deposits has shown that gypsum precipitation also occurred along the Messinian continental margin slope. These findings then question current hypotheses suggesting that gypsum precipitation/preservation only occurred at silled basins or water depths shallower than 200 m.

Acknowledgements

The research leading to these results has received funding from the People Programme (Marie Curie Actions) of the European Union's Seventh Framework Programme FP7/2007–2013/ under REA Grant Agreement No. 290201 MEDGATE. REPSOL-Spain and the *Instituto Geológico y Minero de España-IGME* are thanked for providing access to data and samples. D. Ochoa specially thanks R. Flecker and the MEDGATE team (researchers, staff, partners and associates) for their constructive comments, support and scientific discussions. We acknowledge Bill Ryan, Derek Vance, and two anonymous reviewers for their useful comments, which help improve this manuscript.

Appendix A. Supplementary material

Supplementary material related to this article can be found online at <http://dx.doi.org/10.1016/j.epsl.2015.06.059>.

References

- Acosta, J., Canals, M., Carbó, A., Muñoz, A., Urgeles, R., Muñoz-Martín, A., Uchupi, E., 2004. Sea floor morphology and Plio-Quaternary sedimentary cover of the Mallorca Channel, Balearic Islands, western Mediterranean. *Mar. Geol.* 206, 165–179.
- Alfaro, P., Delgado, J., Estévez, A., Soria, J., Yébenes, A., 2002. Onshore and offshore compressional tectonics in the eastern Betic Cordillera (SE Spain). *Mar. Geol.* 186, 337–349.
- Braga, J.C., Martín, J.M., Riding, R., Aguirre, J., Sánchez-Almazo, I.M., Dinarès-Turell, J., 2006. Testing models for the Messinian salinity crisis: the Messinian record in Almería, SE Spain. *Sediment. Geol.* 188, 131–154.
- CIESM, 2008. The Messinian Salinity Crisis from megadeposits to microbiology—a consensus report. In: Briand, F. (Ed.), CIESM Workshop Monographs. Almería, Spain, p. 168.
- Clauzon, G., Suc, J.-P., Gautier, F., Berger, A., Loutre, M.-F., 1996. Alternate interpretation of the Messinian salinity crisis: controversy resolved? *Geology* 24, 363–366.
- Corbí, H., Soria, J.M., Pina, J.A., 2010. Biostratigrafía basada en foraminíferos planctónicos para el Mioceno superior y Plioceno de la Cuenca del Bajo Segura (Cordillera Bética oriental). *Geogaceta* 48, 71–74.
- Cornée, J.-J., Saint Martin, J.-P., Conesa, G., Münch, P., André, J.-P., Saint Martin, S., Roger, S., 2004. Correlations and sequence stratigraphic model for Messinian carbonate platforms of the western and central Mediterranean. *Int. J. Earth Sci.* 93, 621–633.
- De Lange, G.J., Krijgsman, W., 2010. Messinian salinity crisis: a novel unifying shallow gypsum/deep dolomite formation mechanism. *Mar. Geol.* 275, 273–277.
- Dela Pierre, F., Clari, P., Bernardi, E., Naticchio, M., Costa, E., Cavagna, S., Lozar, F., Lugli, S., Manzi, V., Roveri, M., 2012. Messinian carbonate-rich beds of the Tertiary Piedmont Basin (NW Italy): microbially-mediated products straddling the onset of the salinity crisis. *Palaeogeogr. Palaeoclimatol. Palaeoecol.* 344, 78–93.
- Driussi, O., Maillard, A., Ochoa, D., Lofi, J., Chanier, F., Gaullier, V., Briais, A., Sage, F., Sierro, F., García, M., in press. Messinian Salinity Crisis deposits widespread over the Balearic Promontory: insights from new high-resolution seismic data. *Mar. Pet. Geol.*
- Dronkert, H., 1976. Late Miocene evaporites in the Sorbas basin and adjoining areas. *Mem. Soc. Geol. Ital.* 16, 341–362.
- Ellis, D.V., Singer, J.M., 2007. *Well Logging for Earth Scientists*, 2nd edn. Springer, Netherlands.
- Emeis, K.-C., Robertson, A.H.F., Richter, C., et al., 1996. In: *Proceedings of the Ocean Drilling Program*. In: Initial Reports, vol. 160. College Station, TX, US.
- Fortuin, A., Krijgsman, W., Hilgen, F., Sierro, F., 2000. Late Miocene Mediterranean desiccation: topography and significance of the 'Salinity Crisis' erosion surface on-land in southeast Spain: comment. *Sediment. Geol.* 133, 167–174.
- Ghielmi, M., Minervini, M., Nini, C., Rogledi, S., Rossi, M., 2013. Late Miocene–Middle Pleistocene sequences in the Po Plain–Northern Adriatic Sea (Italy): the stratigraphic record of modification phases affecting a complex foreland basin. *Mar. Pet. Geol.* 42, 50–81.
- Hilgen, F., Krijgsman, W., Langereis, C., Lourens, L., Santarelli, A., Zachariasse, W., 1995. Extending the astronomical (polarity) time scale into the Miocene. *Earth Planet. Sci. Lett.* 136, 495–510.
- Hilgen, F.J., Krijgsman, W., 1999. Cyclostratigraphy and astrochronology of the Tripoli diatomite formation (pre-evaporite Messinian, Sicily, Italy). *Terra Nova* 11, 16–22.
- Hüsing, S., Kuiper, K., Link, W., Hilgen, F., Krijgsman, W., 2009. The upper Tortonian–lower Messinian at Monte dei Corvi (Northern Apennines, Italy): completing a Mediterranean reference section for the Tortonian Stage. *Earth Planet. Sci. Lett.* 282, 140–157.
- Kouwenhoven, T., Seidenkrantz, M.-S., Van der Zwaan, G., 1999. Deep-water changes: the near-synchronous disappearance of a group of benthic foraminifera from the Late Miocene Mediterranean. *Palaeogeogr. Palaeoclimatol. Palaeoecol.* 152, 259–281.
- Krijgsman, W., Fortuin, A., Hilgen, F., Sierro, F., 2001. Astrochronology for the Messinian Sorbas basin (SE Spain) and orbital (precessional) forcing for evaporite cyclicity. *Sediment. Geol.* 140, 43–60.
- Krijgsman, W., Garcés, M., Agustí, J., Raffi, I., Taberner, C., Zachariasse, W., 2000. The 'Tortonian salinity crisis', the eastern Betics (Spain). *Earth Planet. Sci. Lett.* 181, 497–511.
- Krijgsman, W., Hilgen, F., Raffi, I., Sierro, F., Wilson, D., 1999. Chronology, causes and progression of the Messinian salinity crisis. *Nature* 400, 652–655.
- Krijgsman, W., Leewis, M.E., Garcés, M., Kouwenhoven, T.J., Kuiper, K.F., Sierro, F.J., 2006. Tectonic control for evaporite formation in the Eastern Betics (Tortonian; Spain). *Sediment. Geol.* 188, 155–170.
- Laskar, J., Robutel, P., Joutel, F., Gastineau, M., Correia, A., Levrard, B., 2004. A long-term numerical solution for the insolation quantities of the Earth. *Astron. Astrophys.* 428, 261–285.
- Lofi, J., Déverchère, J., Gaullier, V., Gillet, H., Gorini, C., Guennoc, P., Loncke, L., Maillard, A., Sage, F., Thion, I., 2011. Seismic Atlas of the Messinian Salinity Crisis Markers in the Mediterranean and Black Seas. Commission for the Geological Map of the World, Paris, France.
- Lourens, L.J., Antonarakou, A., Hilgen, F., Van Hoof, A., Vergnaud-Grazzini, C., Zachariasse, W., 1996. Evaluation of the Plio-Pleistocene astronomical timescale. *Paleoceanography* 11, 391–413.
- Lugli, S., Manzi, V., Roveri, M., Schreiber, C., 2010. The Primary Lower Gypsum in the Mediterranean: a new facies interpretation for the first stage of the Messinian salinity crisis. *Palaeogeogr. Palaeoclimatol. Palaeoecol.* 297, 83–99.
- Maillard, A., Driussi, O., Lofi, J., Briais, A., Chanier, F., Hübscher, C., Gaullier, V., 2014. Record of the Messinian Salinity Crisis in the SW Mallorca area (Balearic Promontory, Spain). *Mar. Geol.* 357, 304–320.
- Maillard, A., Gorini, C., Mauffret, A., Sage, F., Lofi, J., Gaullier, V., 2006. Offshore evidence of polyphase erosion in the Valencia Basin (Northwestern Mediterranean): scenario for the Messinian Salinity Crisis. In: Rouchy, J.M., Suc, J.-P., Ferrandini, J. (Eds.), *The Messinian Salinity Crisis Revisited, Next Messinian Colloquium*. *Sediment. Geol.* 188–189, 69–91.
- Maillard, A., Mauffret, A., 2013. Structure and present-day compression in the offshore area between Alicante and Ibiza Island (Eastern Iberian Margin). *Tectonophysics* 591, 116–130.
- Manzi, V., Gennari, R., Hilgen, F., Krijgsman, W., Lugli, S., Roveri, M., Sierro, F.J., 2013. Age refinement of the Messinian salinity crisis onset in the Mediterranean. *Terra Nova* 25, 315–322.
- Manzi, V., Roveri, M., Gennari, R., Bertini, A., Biffi, U., Giunta, S., Iaccarino, S.M., Lanci, L., Lugli, S., Negri, A., 2007. The deep-water counterpart of the Messinian Lower

- Evaporites in the Apennine foredeep: the Fananello section (Northern Apennines, Italy). *Palaeogeogr. Palaeoclimatol. Palaeoecol.* 251, 470–499.
- Martín, J., Braga, J.C., 1994. Messinian events in the Sorbas Basin in southeastern Spain and their implications in the recent history of the Mediterranean. *Sediment. Geol.* 90, 257–268.
- Martínez del Olmo, W., 2011. El Messiniense en el Golfo de Valencia y el Mar de Alborán: implicaciones paleogeográficas y paleoceanográficas. *Rev. Soc. Geol. Esp.* 24, 237–257.
- Montadert, L., Sancho, J., Fail, J., Debyser, J., Winnock, E., 1970. De l'âge tertiaire de la série salifère responsable des structures diapiriques en Méditerranée Occidentale (Nord-Est des Baléares). *C. R. Acad. Sci.* 271, 812–815.
- Riding, R., Braga, J.C., Martín, J.M., Sánchez-Almazo, I.M., 1998. Mediterranean Messinian Salinity Crisis: constraints from a coeval marginal basin, Sorbas, southeastern Spain. *Mar. Geol.* 146, 1–20.
- Rogerson, M., Rohling, E., Bigg, G., Ramirez, J., 2012. Paleooceanography of the Atlantic-Mediterranean exchange: overview and first quantitative assessment of climatic forcing. *Rev. Geophys.* 50.
- Roveri, M., Boscolo Gallo, A., Rossi, M., Gennari, R., Iaccarino, S.M., Lugli, S., Manzi, V., Negri, A., Rizzini, F., Taviani, M., 2005. The Adriatic foreland record of Messinian events (central adriatic sea, Italy). *GeoActa* 4, 139–158.
- Roveri, M., Flecker, R., Krijgsman, W., Lofi, J., Lugli, S., Manzi, V., Sierro, F.J., Bertini, A., Camerlenghi, A., De Lange, G., 2014. The Messinian Salinity Crisis: past and future of a great challenge for marine sciences. *Mar. Geol.* 352, 25–58.
- Roveri, M., Gennari, R., Lugli, S., Manzi, V., 2009. The terminal carbonate complex: the record of sea-level changes during the Messinian salinity crisis. *GeoActa* 8, 63–77.
- Roveri, M., Lugli, S., Manzi, V., Schreiber, B.C., 2008. The Messinian sicilian stratigraphy revisited: new insights for the Messinian salinity crisis. *Terra Nova* 20, 483–488.
- Ryan, W., Cita, M.B., 1978. The nature and distribution of Messinian erosional surfaces—indicators of a several-kilometer-deep Mediterranean in the Miocene. *Mar. Geol.* 27, 193–230.
- Ryan, W., Hsü, K., Cita, M., Dumitrica, P., Lort, J., Maync, W., Nesteroff, V., Pautot, G., Stradner, H., Wezel, F., 1973. Initial Reports of the Deep Sea Drilling Project. XIII (Leg 13). US Government Printing Office.
- Ryan, W.B., 2008. Modeling the magnitude and timing of evaporative drawdown during the Messinian salinity crisis. *Stratigraphy* 5, 227–243.
- Sierro, F., Flores, J., Francés, G., Vazquez, A., Utrilla, R., Zamarreño, I., Erlenkeuser, H., Barcena, M., 2003. Orbitally-controlled oscillations in planktic communities and cyclic changes in western Mediterranean hydrography during the Messinian. *Palaeogeogr. Palaeoclimatol. Palaeoecol.* 190, 289–316.
- Sierro, F., Hilgen, F., Krijgsman, W., Flores, J., 2001. The Abad composite (SE Spain): a Messinian reference section for the Mediterranean and the APTS. *Palaeogeogr. Palaeoclimatol. Palaeoecol.* 168, 141–169.
- Sierro, F.J., Ledesma, S., Flores, J.-A., Torrecusa, S., del Olmo, W.M., 2000. Sonic and gamma-ray astrochronology: cycle to cycle calibration of Atlantic climatic records to Mediterranean sapropels and astronomical oscillations. *Geology* 28, 695–698.
- Soria, J., Alfaro, P., Fernández, J., Viseras, C., 2001. Quantitative subsidence-uplift analysis of the Bajo Segura Basin (eastern Betic Cordillera, Spain): tectonic control on the stratigraphic architecture. *Sediment. Geol.* 140, 271–289.
- Soria, J., Caracuel, J., Yébenes, A., Fernández, J., Viseras, C., 2005. The stratigraphic record of the Messinian salinity crisis in the northern margin of the Bajo Segura Basin (SE Spain). *Sediment. Geol.* 179, 225–247.
- Soria, J.M., Caracuel, J.E., Corbí, H., Dinarès-Turell, J., Lancis, C., Tent-Manclús, J.E., Viseras, C., Yébenes, A., 2008. The Messinian–early Pliocene stratigraphic record in the southern Bajo Segura Basin (Betic Cordillera, Spain): implications for the Mediterranean salinity crisis. *Sediment. Geol.* 203, 267–288.